Time-resolved photoluminescence in nitrogen-doped $GaAs_{1-x}P_x$

1994 J. Phys.: Condens. Matter 6 10377

(http://iopscience.iop.org/0953-8984/6/47/020)

J. Phys.: Condens. Matter 6 (1994) 10377–10390. Printed in the UK

Time-resolved photoluminescence in nitrogen-doped $GaAs_{1-x}P_x$

A Meftah†, M Oueslati† and C Benoit à la Guillaume‡

† *Laboratoire de Spectroscopie Moléculaire, Département de Physique, Faculté des Sciences*, Tunis-1060, Tunisia

‡ Groupe de Physique des Solides de l'Ecole Nationale Supérieure, Université Paris 7, Tour 23, 2 Place Jussieu, 75251 Paris 05, France

Received 6 December 1993, in final form 5 August 1994

Abstract. An experimental time-resolved photoluminescence (PL) study on nitrogen-doped $GaAs_{1-x}P_x$ ($x = 0.59$) at $T = 2$ K shows a non-exponential decay of emission intensity. The nitrogen bound exciton lifetime is relatively large, 0.2–1 μs. The shift to lower energies of the PL band during the decay shows that the transfer rate W_T varies with the nitrogen level energy. To describe the experimental observations, a simple calculation model of the emission intensity is used. In this model, we consider a distribution of zero-phonon radiative recombination rates W_R and a transfer rate W_T obeying the equation $[\![d\{\log[WT(E)]\}/dE]\!]_{E_\mu} = \text{constant}$ (E_μ is the mobility edge).

1. Introduction

In indirect-gap $GaAs_{1-x}P_x$ alloys ($x > 0.46$), nitrogen impurities create a distribution of N_X levels which appears in photoluminescence (PL) spectra as a broad band for arsenic-rich samples [1–5]. This broadening is due to a disordered composition and can be described by the $x(1-x)$ law [2, 3]. Several workers [3, 5–7] have shown that the maximum of the PL band is shifted to lower energies compared with that of the N_X distribution levels. At resonant excitation, the Raman peaks of both the Γ and the X points of the Brillouin zone (BZ) are more predominant than the PL band [1–3].

Time-resolved studies [8–10] of resonant Raman scattering (RRS) and resonant photoluminescence (RPL) on the N_X band provide competition between radiative recombination at a rate W_R and energy transfer at a rate $W_T(E)$ toward N_X states with a Gaussian distribution.

In this paper, we present in section 2 the RRS and RPL experimental results and we propose in section 3 a model calculation of time-resolved emission intensities provided that the shift of the PL band is fixed by the mobility edge (ME) E_μ where $W_T(E = E_\mu) = W_R$.

2. Experimental details

The sample used is an epitaxial layer grown on a GaP substrate. The nitrogen concentration is of the order of 10^{18} atom cm^{-3}. The sample is cooled by immersion in superfluid helium. At this temperature $T = 2$ K, the indirect-gap energy of $GaAs_{0.41}P_{0.59}$ is $E_g^x = 2.147$ eV (17 318 cm^{-1}).

The experimental set-up is shown in figure 1. The excitation energies are selected from a dye laser using rhodamine 6G pumped with an ionized argon laser operating at an

0953-8984/94/4710377+14$19.50

energy of 2.41 eV. Pulses with a convenient repetition rate (100 kHz) are obtained from an acousto-optical modulator. The pulse duration and power density are 50 ns and 3 W cm^{-2}, respectively. The sample luminescence is analysed with a double monochromator equipped with a cooled GaAs photomultiplier and processed in the single-photon-counting mode using a microcomputer-controlled time-to-amplitude converter.

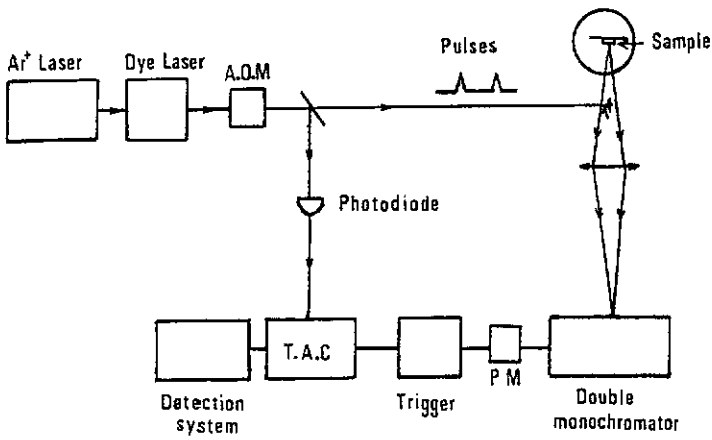

Figure 1. Experimental set-up: AOM, acoustic-optical modulator; TAC, time-to-amplitude converter; PM, photomultiplier.

Figures 2 and 3 show the PL spectra of nitrogen-doped $GaAs_{1-x}P_x$ ($x = 0.59$) for various delays and for the excitation energies $E_i = 2.068$ eV (16 681 cm^{-1}) and $E_i = 2.047$ eV (16 512 cm^{-1}). In figure 2, curve a, and figure 3, curve a, peaks labelled 1, 2, 3, 4 and 5 are more predominant than the PL band, move with the laser energy and disappear at long delay times. They are attributed to resonant Raman emission with TA^X, LA^X, LO^{loc}, TO^Γ and LO^Γ phonons, respectively [1] (table 1). Relative to the PL band, the peak intensities decrease with increasing delay. These peaks are still observed in figure 2, curves b and c, and figure 3, curves b and c. Non-resonant Raman processes are very fast and the intermediate states are virtual. In resonant Raman processes, the exciton lifetime is increased by the stability of the intermediate state, causing competition between the resonant Raman and PL processes. For increasing delay time, the Raman peak intensities vanish, the relative intensities due to recombination from high N_X levels decrease and the maximum of the PL band is shifted to lower energies. This reflects the exciton transfer of N_X bound excitons between levels of the density-of-states band.

Table 1. Raman emission peaks.

Peak	Phonon	E (meV)
1	TA^X	12.5
2	LA^X	26
3	LO^{loc}	33.6
4	TO^Γ	45.9
5	LO^Γ	48.2

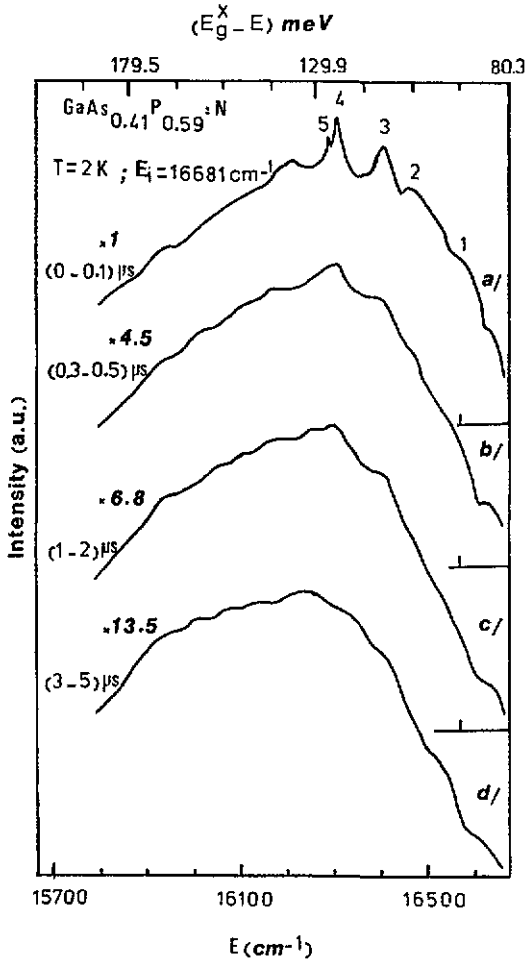

Figure 2. Time-resolved PL spectra of $GaAs_{0.41}P_{0.59}$:N at $T = 2$ K under pulsed excitation energy E_i where $E_p = E_g^X - E_i = 79$ meV (a.u., arbitrary units).

Experimental results show that the PL band shift ΔE is independent of excitation energy E_i but varies with the delay time. Table 2 give sthe experimental values of ΔE for different delay times R at excitation energy $E_i = 2.068$ eV. (ΔE is measured with respect to the excitation spectra maximum for $x = 0.59$ deduced from [5].)

Table 2. Experimental shifts ΔE for various delay times R.

R (μs)	ΔE (meV)
0–0.1	39.5
0.3–0.5	47.8
1–2	49
3–5	65.1

Figure 4 shows the PL spectra for different excitation energies and for the same short

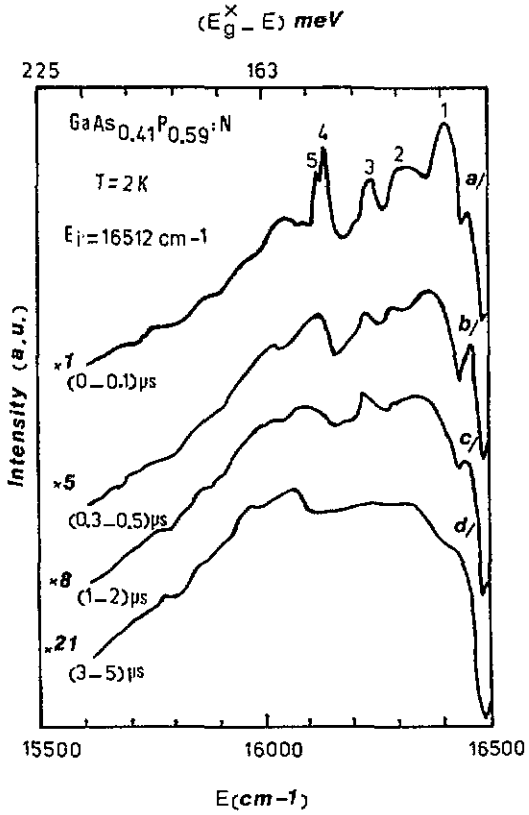

Figure 3. Time-resolved PL spectra of $GaAs_{0.41}P_{0.59}$:N at $T = 2$ K under pulsed excitation energy E_i where $E_p = E_g^x - E_i = 100$ meV (a.u., arbitrary units).

delay time $R = 0$–0.1 μs. Peaks corresponding to the fast processes are present. For large delay times $R = 3$–5 μs, the phonon peaks disappear and the PL band is simply due to recombination of excitons with a long lifetime (figure 5). When the excitation energy decreases, the intensity of the resonant Raman peaks increases with respect to the PL band. For lower excitation energies, the spectra are dominated by Raman peaks.

In figure 6, we have reported the time emission intensity decay ($\log[I(t)/I_0]$) from three energy windows, each of 5 meV width, and centred at 11.9, 26.8 and 34.2 meV below the excitation energy 2.068 eV. (I_0 is the maximum of the intensity $I(t)$). For short delay times the decay is dominated by fast processes and the lifetime is nearly the same for all levels. For large delay times the lifetime is of the order of 700 ns and it increases with increasing depth of the N_x level.

3. Theoretical model

For sufficiently large delay times, fast processes vanish and the PL is mainly due to recombination of nitrogen bound excitons. Excitons can either recombine with a probability W_R or transfer towards any exciton states of lower energy with a probability W_T (figure 7(a)).

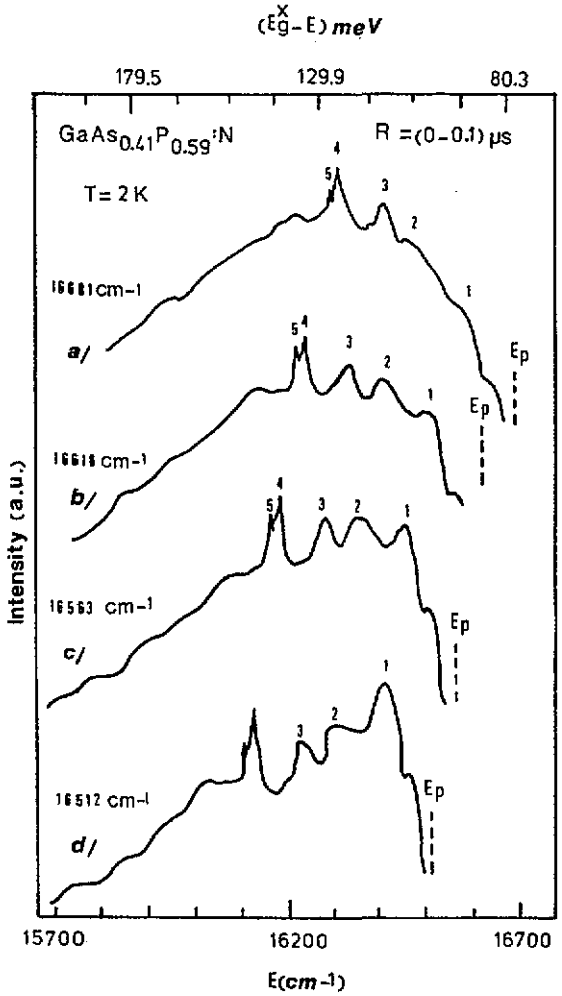

Figure 4. PL spectra of $GaAs_{0.41}P_{0.59}$:N at $T = 2$ K, for a delay time $R = 0$–0.1 μs and for various excitation energies E_i where $E_p = E_g^x - E_i$ (a.u., arbitrary units): curve a, $E_p = 79$ meV; curve b, $E_p = 87$ meV; curve c, $E_p = 93$ meV; curve d, $E_p = 100$ meV.

We consider a pulsed excitation with energy E_p in resonance with a nitrogen level labelled P. The energy origin is taken at the minimum of the exciton conduction band (E_g^x) at the X point of the BZ. Let T be the period of the pulsed excitation and τ_0 the pulse width (figure 7(b)). The generation rate $G(t)$ due to excitation of level P will be as follows:

$$G(t) = \begin{cases} G_0 \\ 0 \end{cases} \quad \text{for} \quad \begin{cases} -\tau_0 < t \leqslant 0 \\ t > 0. \end{cases}$$

For a resonant level P the exciton population obeys the equations

$$\frac{dn_p(t)}{dt} = \begin{cases} G_0 - a_p n_p(t) \\ -a_p n_p(t) \end{cases} \quad \text{for} \quad \begin{cases} -\tau_0 < t \leqslant 0 \\ t > 0. \end{cases} \tag{1}$$

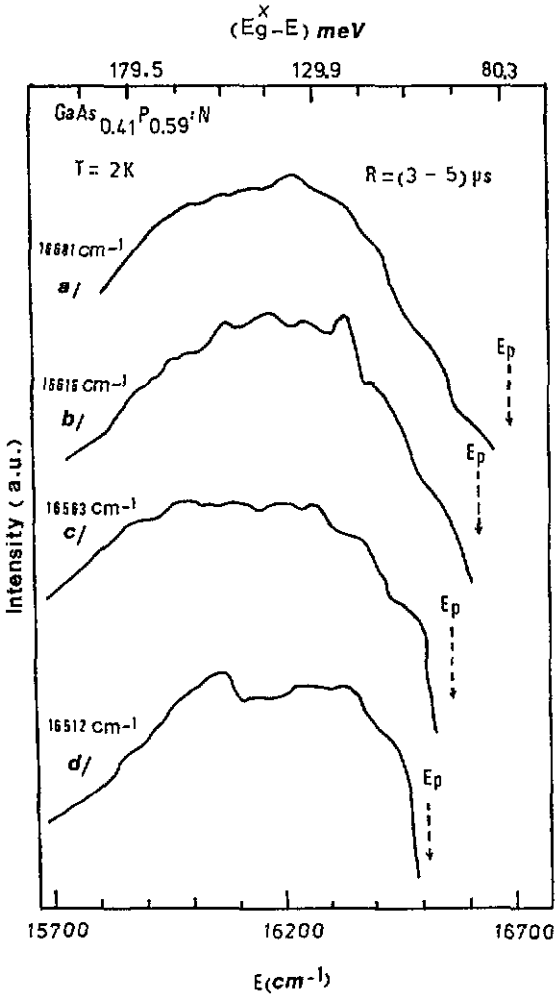

Figure 5. The same as for figure 2 but for a delay time $R = 3$–5 μs (a.u., arbitrary units).

For any level labelled i located below the resonant level P, the exciton population obeys the equation

$$\frac{dn_i(t)}{dt} = -a_i n_i(t) + \sum_{j=p}^{j=i-1} W_T(j,i) n_j(t). \tag{2}$$

a_i is the sum of the radiative recombination rate $W_R(i)$ and the transfer rate $W_T(i)$ from level i:

$$a_i = W_R(i) + W_T(i). \tag{3}$$

$W_T(j,i)$ is the transfer rate from level j to level i. At low temperatures, transfer to upper levels is negligible. $W_T(j,i)$ depends on $W_T(j)$ and the density of states at level i. It is

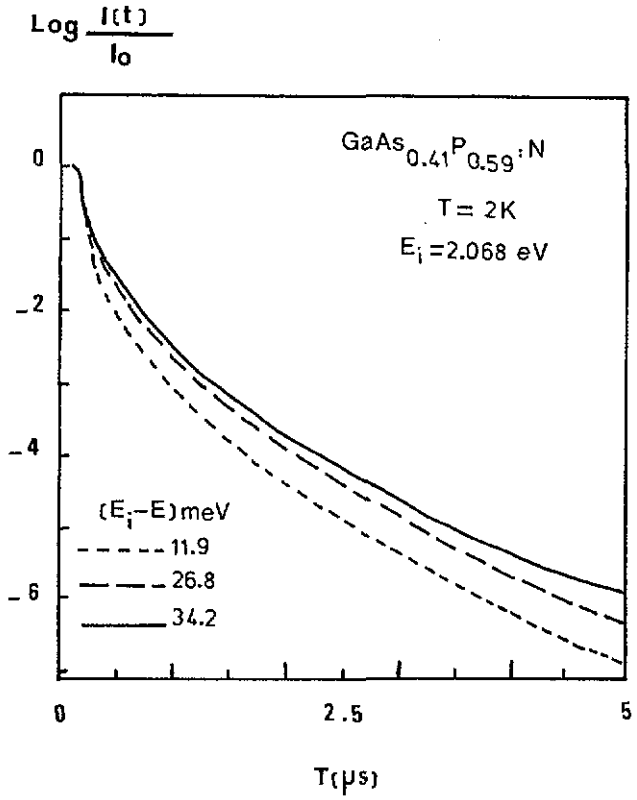

Figure 6. Emission intensity decay from three energy windows, each of 5 meV width and centred at 11.9, 26.8 and 34.2 meV below the excitation energy $E_i = 2.063$ eV.

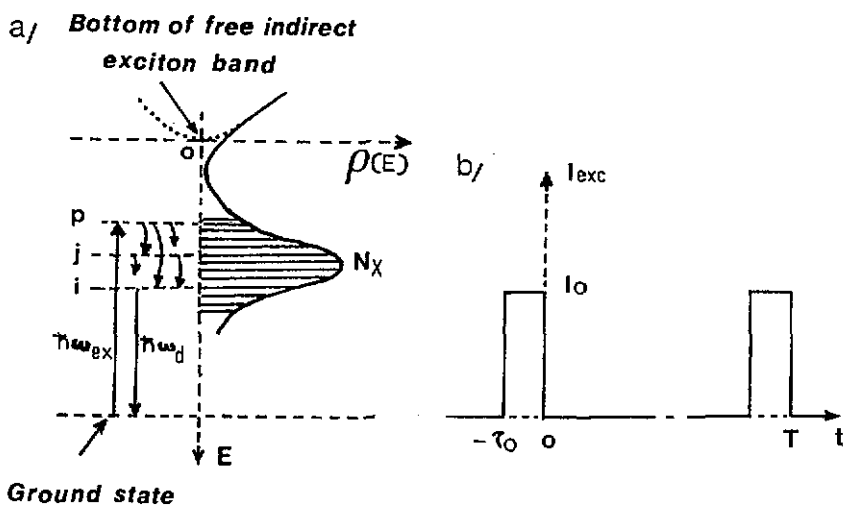

Figure 7. (*a*) Density of states of the N_x band: schematic representation of exciton transfer and recombination processes. (*b*) Pulsed excitation.

given by

$$W_T(j,i) = K\,W_T(j)\rho(i) \Big/ \sum_{i>j} \rho(i) \tag{4}$$

$$W_T(j) = \sum_{i>j} W_T(j,i). \tag{5}$$

K is a normalizing constant and is determined by equation (5).

As in [3,4,8,11] the density of states is taken as Gaussian, i.e. $\rho = \rho_0 \exp[-[(E_i - E_0)/\Delta]^2\}$; hence

$$W_T(j,i) = \frac{\Delta}{\sqrt{\pi}} \frac{W_T(j)\exp\{-[(E_i - E_0)/\Delta]^2\}}{\operatorname{erfc}[(E_j - E_0)/\Delta]} \tag{6}$$

where erfc is the complementary error function.

As in [9, 10], we take the recombination rate W_R to be independent of the energy levels and we define a ME with an energy E_μ as follows:

$$\begin{aligned} W_T(E) &> W_R \qquad \text{for} \qquad E < E_\mu \\ W_T(E) &= W_R \qquad \text{for} \qquad E = E_\mu \\ W_T(E) &< W_R \qquad \text{for} \qquad E > E_\mu. \end{aligned} \tag{7}$$

$W_T(E)$ is characterized by its logarithmic derivative:

$$\alpha = \left(\frac{\mathrm{d}\{\log[W_T(E)]\}}{\mathrm{d}E}\right)_{E_\mu}. \tag{8}$$

Hence

$$W_T(E) = W_R \exp[\alpha(E_\mu - E)]. \tag{9}$$

The parameter α is related to the localization length of state E and fixes the energy dependence of transfer inside the N_x density band.

For the steady-state case the solutions of (1) and (2) are

$$\begin{aligned} n_p &= \frac{G_0}{a_p} \\ n_i &= \frac{1}{a_i} \sum_{j=p}^{j=i-1} W_T(j,i) n_j. \end{aligned} \tag{10}$$

For $-\tau_0 < t \leqslant 0$ the solutions of equations (1) and (2) could be written as

$$\begin{aligned} n_p(t) &= A(p, p-1) + A(p,p)\exp[-a_p(t+\tau_0)] \\ n_i(t) &= \sum_{l=p-1}^{l=i-1} A(i,l)\exp[-a_l(t+\tau_0)] + A(i,i)\exp[-a_i(t+\tau_0)] \end{aligned} \tag{11}$$

with

$$A(p, p-1) = \frac{G_0}{a_p} \qquad A(p, p) = -\frac{G_0}{a_p}.$$

The coefficients $A(i, j)$ obey the equalities

$$\begin{aligned} A(i, i) &= -\sum_{j=p}^{j=i-1} W_T(j, i) \sum_{s=p-1}^{s=j} \frac{A(j, s)}{a_i - a_s} \qquad \text{for } i \geqslant p+1 \\ A(i, p-1) &= \sum_{l=p}^{l=i-1} W_T(l, i) A(l, p-1) \\ A(i, l) &= \frac{1}{a_i - a_l} \sum_{r=l}^{r=i-1} W_T(r, i) A(r, l). \end{aligned} \tag{12}$$

For $t > 0$ the solutions of (1) and (2) are

$$n_p(t) = B(p, p) \exp(-a_p t) \tag{13}$$

$$n_i(t) = \sum_{j=p}^{j=i-1} B(i, j) \exp(-a_j t) + B(i, i) \exp(-a_i t). \tag{14}$$

The continuity of the solutions at $t = 0$ allows us to determine the relation between the coefficients $B(i, j)$ and $A(i, j)$:

$$\begin{aligned} B(p, p) &= n_p(0) = \frac{G_0}{a_p}[1 - \exp(-a_p \tau_0)] \\ B(i, i) &= n_i(0) - \sum_{j=p}^{j=i-1} B(i, j) \qquad \text{for } i \geqslant p+1 \\ n_i(0) &= A(i, p-1) + \sum_{l=p}^{l=i} A(i, l) \exp(-a_l \tau_0) \\ B(i, j) &= \frac{1}{a_i - a_j} \sum_{r=j}^{r=i-1} W_T(r, i) B(r, j). \end{aligned} \tag{15}$$

To calculate the emission intensity $I(E, t)$ from a level i with an energy E in the density of states band at time t, we consider that, in $GaAs_{1-x}P_x$:N alloys, the exciton sees a potential fluctuation due to the disordered composition which mixes the Γ and X states. So, W_R is not constant and is described by a probability distribution calculated by Klein *et al* [12] and given by

$$P(W_R) = \frac{1}{\langle W_R \rangle} \exp\left(-\frac{W_R}{\langle W_R \rangle}\right) \tag{16}$$

where $\langle W_R \rangle$ is the mean phonon-less radiative rate. $I(E, t)$ is given by

$$I(E, t) = \int_0^\infty n(E, W_R, t) P(W_R) W_R \, dW_R. \tag{17}$$

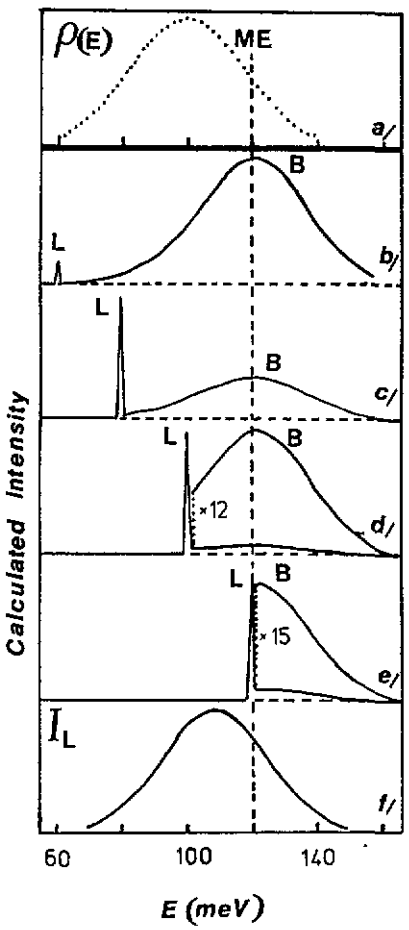

Figure 8. (*a*) Density of states: calculated emission inetnsity in the steady-state case for various excitation energies E_i where $E_p = E_g^x - E_i$: (*b*) $E_p = 60$ meV; (*c*) $E_p = 80$ meV; (*d*) $E_p = 100$ meV; (*e*) $E_p = 120$ meV; (*f*) intensity variation of the resonant line L with excitation energy.

For the resonant level P with energy E_p, the equation (13) gives

$$I(E_p, t) = \frac{G_0\langle W_R\rangle}{\langle a_p\rangle}\left(\frac{1}{(1+\langle a_p\rangle t)} - \frac{1}{(1+\langle a_p\rangle(t+\tau))}\right). \tag{18}$$

For one level with energy $E = E_i$, equation (14) gives

$$I(E,t) = \sum_{E_l=E_p-1}^{E_l=E_i} A(i,l)\frac{\langle W_R\rangle}{(1+\langle a_l\rangle\tau+\langle a_i\rangle t)}\frac{\langle W_R\rangle}{1-\exp[-(\langle a_p\rangle\tau)]}\sum_{E_j=E_p}^{E_j=E_i-1} B(i,j)\left(\frac{1}{1+\langle a_j\rangle t}\right.$$
$$\left. - \frac{1}{1+\langle a_i\rangle t} + \frac{1}{1+\langle a_p\rangle\tau+\langle a_i\rangle t} - \frac{1}{1+\langle a_p\rangle\tau+\langle a_j\rangle t}\right) \tag{19}$$

where

$$\langle a_i\rangle = \langle W_R\rangle\{1+\exp[\alpha(E_\mu - E_i)]\}.$$

Equations (18) and (19) give for chosen excitation energies E_p

(i) the emission spectra $I = f(E)$ at different times t and
(ii) the intensity decay $I = f(t)$ for different energies E.

The calculations are processed by computer. The energy $E_0 = 100$ meV of the maximum of the density of states band is deduced from [5]. The adjusted values $\Delta = 25$ meV, $\alpha = 0.05$ meV^{-1}, $E_\mu = 120$ meV and $W_R \approx 2.5 \times 10^6$ s^{-1} give good agreement with the experimental results.

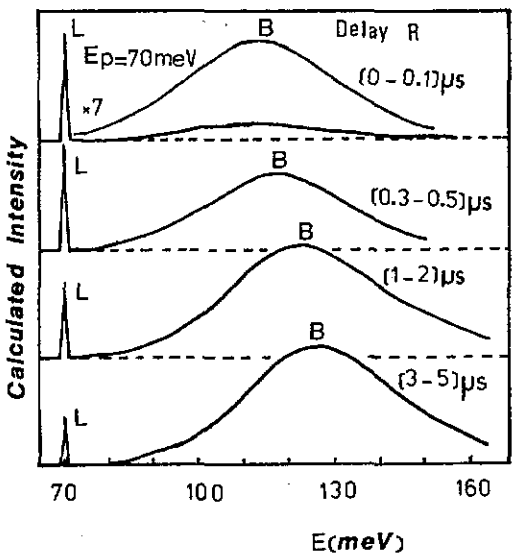

Figure 9. Time-resolved calculated emission intensity for various delay times for the excitation energy E_i where $E_p \approx E_g^x - E_i = 70$ meV.

Table 3. Calculated shifts ΔE for various delay times R.

R (μs)	ΔE (meV)
0–0.1	13
0.3–0.5	18
1–2	24
3–5	27

4. Discussion

The calculated emission spectra are formed by the superposition of a line L and a band B. Band B corresponds to the experimental N_x PL band. Line L is due to emission from the resonant level P. This line traduces the Raman diffusion with one phonon (TA^X, LA^X, LO^{loc}, TO^Γ or LO^Γ).

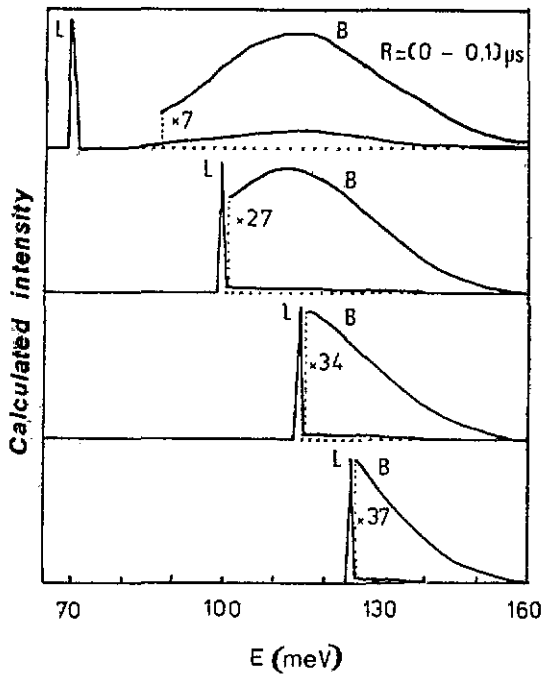

Figure 10. Calculated emission intensity for a delay time $R = 0$–0.1 μs and for various excitation energies E_i where $E_p = E_g^x - E_i$: (*a*) $E_p = 70$ meV; (*b*) $E_p = 100$ meV; (*c*) $E_p = 115$ meV; (*d*) $E_p = 125$ meV.

4.1. Steady-state case

For continuous excitation, the maximum of band B of the calculated spectra is shifted to lower energy than the maximum of the density of states band. The shift is 22 meV (figure 8). Wolford *et al* [3] estimate a shift of 15 meV or more for a composition near mid-alloy. Marjette *et al* [5] have found an experimental value of 27 meV. The shift is attributed to exciton transfer to lower energies in the density of states band $\rho(E)$. In our model the shift is described by the existence of a ME which depends on the three parameters α, E_μ and (W_R) determining the transfer rate $W_T(E)$ (equation (9)).

According to our experimental results [1], the shift is independent of the energy E_p of the excited level. The intensity I_L of line L increases with increasing level depth and has a maximum near the ME with energy E_μ (figure 8, curve f).

4.2. Time-dependent mode

The shape of band B of the calculated spectra depends on the excitation energy level E_p and delay time R from the end of the excitation pulse. The values of E_p and R used take into account the experimental values to allow a comparison between calculated and experimental results.

For the same excitation energy E_p (figure 9), the shift ΔE increases with increasing delay time. The shifts calculated for different delay times are given in table 3. These values are smaller than the experimental data given in table 2. The superposition of the phonon replica on the N_x band in the experimental spectra gives a resulting band with an energy

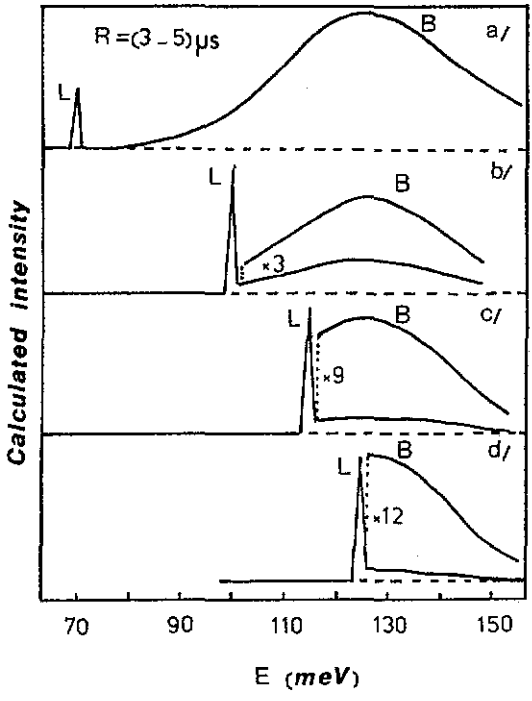

Figure 11. The same as for figure 8, but for a delay time $R = 3$–5 μs.

maximum deeper in the density-of-states band and enhances the shift. The additional shift is estimated by Mariette *et al* [5] to be about 10 meV.

For the same delay the shift is independent of the excitation energy (figures 10 and 11). When the delay time increases, the intensity of line L decreases more rapidly than does the intensity of band B. Line L describes the time behaviour of the experimental Raman lines.

According to the experimental results, the time decay of the calculated intensity $I(E, t)$ (figure 12) is non-exponential. The non-exponential decay is well described by the distribution of radiative decay rates W_R due to the disordered composition in $GaAs_{1-x}P_x$:N alloys (equation (16)). The time decay of the intensity included both radiative and transfer rates: $W_R + W_T(E) = 1/\tau_a$. The apparent lifetime τ_a increases with increasing level depth in the density of states band and tends for deep levels to the average radiative lifetime $\tau_R = \langle W_R \rangle^{-1}$.

5. Conclusion

The time-resolved emission intensity has been shown to be a superposition of RRS spectra and PL spectra. The lifetime of the resonant peaks increases on approaching the PL band lifetime, when probing deeper states in the N_x density of states.

The calculation model of the emission band intensity $I(E, t)$ from N_x exciton states reproduces our previous experimental results and describes very well the evolution of $I(E, t)$ with various experimental parameters.

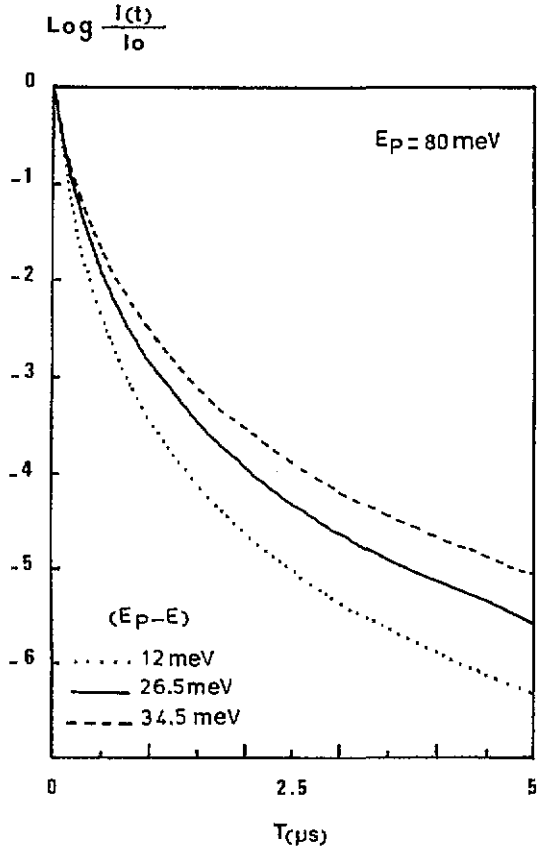

Figure 12. Calculated emission intensity decay from three energy windows each of 2 meV width and located at 12, 26.5 and 34.5 meV below the excitation energy $E_p = 80$ meV.

The theoretical model has shown that the apparent lifetime depends on transfer processes. This model shows that the shift in the PL band maximum is due to the competition between radiative and transfer processes. The shift value is determined by the ME energy E_μ.

References

[1] Meftah A, Oueslati M and Zouaghi M 1987 *Solid State Commun.* **62** 305
[2] Wolford D J, Streetman B G, Shui Lai and Klein M V 1979 *Solid State Commun.* **32** 51
[3] Wolford D J, Streetman B G and Thompson J 1980 *J. Phys. Soc. Japan* **49** 223
[4] Wolford D J, Hsu W Y, Dow J D and Streetman B G 1979 *J. Lumin.* **18–19** 863
[5] Mariette H, Chevalier J and Leroux-Hugon P 1980 *Phys. Rev.* B **21** 5706
[6] Mariette H and Chevalier J 1979 *Solid State Commun.* **29** 263
[7] Collet J H, Kash J A, Wolford D J and Thompson J 1983 *J. Phys. C: Solid State Phys.* **16** 1283
[8] Gershoni D, Cohen E and Arsa R 1986 *Phys. Rev. Lett.* **56** 2211
[9] Oueslati M, Benoit à la Guillaume C and Zouaghi M 1988 *Phys. Rev.* B **37** 3037
[10] Oueslati M, Benoit à la Guillaume C and Zouaghi M 1989 *J. Phys.: Condens. Matter* **1** 7705
[11] Kash J A 1984 *Phys. Rev.* A **29** 7069
[12] Klein M V, Sturge M D and Cohen E 1982 *Phys. Rev.* B **25** 4331